

CRYSTALLOGRAPHY OF PREFERRED GROWTH IN LEAD-TIN ALLOYS

David Paul Mourer

MASTER

M. S. Thesis Submitted to Iowa State University

Ames Laboratory, ERDA
Iowa State University
Ames, Iowa 50011

Date Transmitted: June 1976

—NOTICE—

This report was prepared as an account of work sponsored by the United States Government. Neither the United States nor the United States Energy Research and Development Administration, nor any of their employees, nor any of their contractors, subcontractors, or their employees, makes any warranty, express or implied, or assumes any legal liability or responsibility for the accuracy, completeness or usefulness of any information, apparatus, product or process disclosed, or represents that its use would not infringe privately owned rights.

PREPARED FOR THE U.S. ENERGY RESEARCH AND DEVELOPMENT
ADMINISTRATION UNDER CONTRACT NO. W-7405-eng-82

DISTRIBUTION OF THIS DOCUMENT IS UNLIMITED

by

DISCLAIMER

This report was prepared as an account of work sponsored by an agency of the United States Government. Neither the United States Government nor any agency Thereof, nor any of their employees, makes any warranty, express or implied, or assumes any legal liability or responsibility for the accuracy, completeness, or usefulness of any information, apparatus, product, or process disclosed, or represents that its use would not infringe privately owned rights. Reference herein to any specific commercial product, process, or service by trade name, trademark, manufacturer, or otherwise does not necessarily constitute or imply its endorsement, recommendation, or favoring by the United States Government or any agency thereof. The views and opinions of authors expressed herein do not necessarily state or reflect those of the United States Government or any agency thereof.

DISCLAIMER

Portions of this document may be illegible in electronic image products. Images are produced from the best available original document.

NOTICE

This report was prepared as an account of work sponsored by the United States Government. Neither the United States nor the United States Energy Research and Development Administration, nor any of their employees, nor any of their contractors, subcontractors, or their employees, makes any warranty, express or implied, or assumes any legal liability or responsibility for the accuracy, completeness, or usefulness of any information, apparatus, product or process disclosed, or represents that its use would not infringe privately owned rights.

Available from: National Technical Information Service
U. S. Department of Commerce
P.O. Box 1553
Springfield, VA 22161

Price: Microfiche \$2.25

Crystallography of preferred growth in lead-tin alloys

by

David Paul Mourer

A Thesis Submitted to the
Graduate Faculty in Partial Fulfillment of
The Requirements for the Degree of
MASTER OF SCIENCE

Department: Materials Science and Engineering

Major: Metallurgy

Approved:

John Verhaegen
In Charge of Major Work

D. L. Miller
For the Major Department

M. J. Ulm
For the Graduate College

Iowa State University
Ames, Iowa

1976

TABLE OF CONTENTS

	Page
ABSTRACT	iii
INTRODUCTION	1
EXPERIMENTAL APPARATUS AND PROCEDURES	11
RESULTS AND DISCUSSION	25
SUMMARY	58
BIBLIOGRAPHY	60
ACKNOWLEDGEMENTS	63

v

ABSTRACT*

The preferred growth of the lead-tin eutectic alloy has been studied by use of electron channeling techniques in a scanning electron microscope. Four distinct crystallographic modes have been found to exist depending on the imposed growth velocity. The extent of the range of the stability of each mode was experimentally determined in a directional solidification apparatus and rationalized in terms of simple physical reasoning. Microstructural observations are discussed in terms of the nature of the extent of the stability of the various crystallographic relationships.

Lamellar spiraling about the growth direction was found to occur in one crystallographic mode and the parameters controlling it, growth velocity and temperature gradient, have been investigated. The rate of lamellar spiraling was found to increase by increasing solidification rate or temperature gradient.

Considering the data as a whole, the study suggests that considerably more control over the microstructural and crystallographic characteristics of a eutectic structure is possible than was previously believed.

*USERDA Report IS-T-718. This work was performed under Contract W-7405-eng-82 with the Energy Research and Development Administration.

INTRODUCTION

In recent years a considerable number of investigations have dealt with the development of preferred crystallographic relationships in directionally solidified alloys particularly two phase lamellar eutectics. Since 1935 due to the work of Straumanns and Brakss (28) it has been known that lamellar eutectics solidify with a preferred crystallography but it is only in the past ten years that significant advances in experimental techniques have permitted detailed studies of the origin and development of a preferred eutectic crystallography. (Since it is beyond the scope of this paper to present a detailed summary of the history of investigations on eutectic alloys the reader is referred to an excellent review article by Hogan et al. (16)).

At this point let us digress a little to familiarize the reader with some of the topological parameters of a eutectic microstructure. A typical microstructure is pictured in Figure 1. The growth direction is normal to the micrograph and one can easily discern the alternating lamellae or "plates" of each phase. It is also clearly evident that the lamellae are not continuous. The termination of a lamellae is termed a lamellar fault. When a number of adjacent lamellae terminate all along a line this trace is evidence of a mismatch surface. A mismatch surface generally lies normal to the lamellae and parallel to the growth direction. The edge

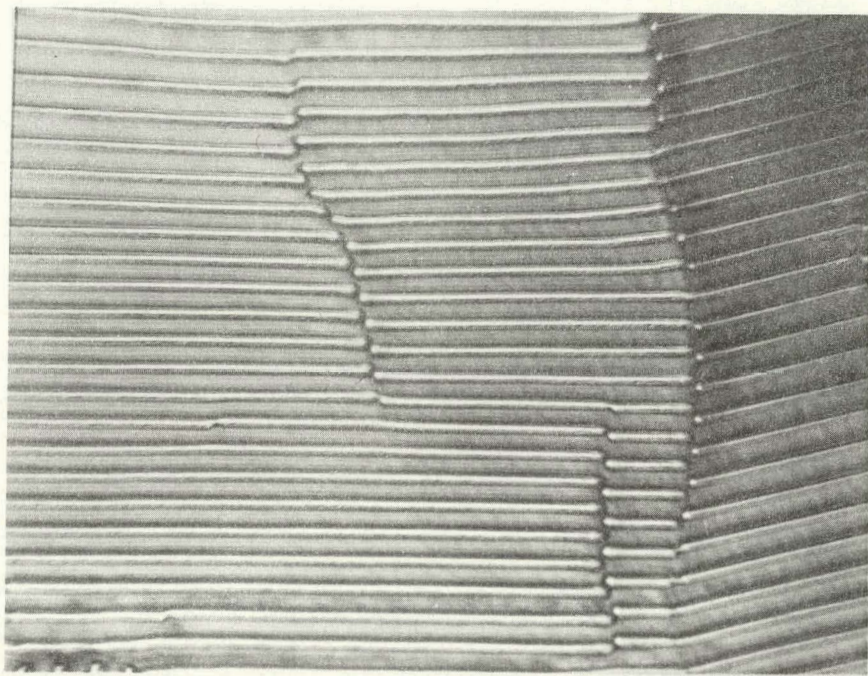


Fig. 1. A typical faulted Pb-Cd eutectic microstructure.
Growth normal to the micrograph. 1000X

of a mismatch surface is not well defined; they simply fade out. If a mismatch surface is merely a displacement of the lamellae, that is if there are equal numbers of lamellae on both sides, it is termed a no-net fault. If, however, the number on one side differs from that on the other it is termed a net fault. Movement of net faults has been proposed to account for the ability of the microstructure to change the lamellar spacing in response to changes in growth rate.

Now let us move on to consider some general concepts of eutectic growth and the development of a preferred crystallography. Lamellar growth is favored by short diffusion distances at the advancing solid-liquid interface but the plate like structure is characterized by a large area of interface per unit volume of material. Thus stabilization of the lamellar structure would occur if growth conditions permitted the selection of a low energy interface. The findings of consistent orientation relationships in many eutectic systems (3,4,5,15,17,18,22) would lead to the conclusion that this does occur and many mechanisms for orientation changes have been proposed to play a role in the selection process (16). In addition to the orientation changes for the selection of a low energy interface each phase will be striving to grow in a favored crystallographic direction. Thus the final preferred crystallographic relationship should be a compromise between maintaining a low energy interface and growth in preferred crystallographic directions.

A complex analysis by Fletcher and Adamson (13) predicts that interfacial energy will vary periodically when the relationship between the interfacial and crystal orientations is varied systematically. Intuitively one realizes that the interfacial energy is a complex function of the five degrees of crystallographic freedom of the interfacial planes. Whenever the lattice parameters, symmetry and orientation of the two crystals give a high percentage of atomic coincidences across the interface a minimum energy configuration will occur. Such a circumstance would produce a minima or perhaps a cusp in an energy versus orientation plot. Physically then, any grain whose crystallographic orientation fell within the width of the minima would experience a driving force towards the minimum energy configuration. Any movement of lamellar faults or crystallographic orientation changes which tended towards this configuration would be stabilized allowing progressive changes to occur slowly as growth proceeded. Let us now consider the actual shape of the energy versus orientation curve. If the minima in the energy versus orientation curve were a sharp cusp one would expect the lamellae to be rigidly parallel and fixed crystallographically since any deviation from the preferred orientation would experience a rapid increase in energy. If the orientation corresponds to a gentle minimum in the curve the driving force maintaining the precise details of the orientation relationship would not be as great and one would expect to find greater variation in the crystal-

PAGES 5 to 6

WERE INTENTIONALLY
LEFT BLANK

habit plane. If the habit plane was $(\bar{1}018)$ Zn the grain was dextro-rotary but if it was $(10\bar{1}8)$ the grain would be laevo-rotary. Their work also indicated that fault density and the range of misorientations decreased with increasing temperature gradient, and that the rate of the lamellar spiraling also decreased with the decrease in fault density and range of misorientations. The applicability of these findings to the lead-tin system may be somewhat in question for two reasons. Unfortunately Hopkins and Steward did not confirm that the lamellar spiraling they studied involved no orientation changes as was the case with the Al-Zn eutectic (nor did they show that it was the same crystallography previously found by Hopkins and Kraft (18)). Secondly, Double typically found the lamellae inclined at up to 25° to the growth direction, a complication not mentioned in previous lead-tin crystallographic studies. In any event it is clear from these studies that the lamellar spiraling phenomena was inherent in the growth process and not a transient phenomena.

In spite of the advances in experimental techniques there is considerable disagreement in the literature over the details of the preferred eutectic crystallography in a given system. A prime example of this is the lead-tin eutectic where depending on the solidification conditions various crystallographic relationships have been reported (17,25,29). In light of the apparent contradictions in the literature over eutectic crystallographic relationships it

might prove beneficial to summarize briefly the assumptions most previous investigators have made as a basis to their work and also any limitations imposed on their experiments due to the nature of the techniques employed. The major experimental limitation was inherent in the X-ray analysis most authors have relied upon (24). Texture X-ray analysis when applied to the determination can only be an averaging technique and unless great care is exercised the analysis will tend to obscure true variations in eutectic crystallography. A second drawback to X-ray analysis is that the relative crystallography found by the X-ray analysis must be correlated to growth directions and interfacial habit plane measurements determined independently by optical microscopy. This procedure introduces additional experimental error into the findings of the study. Also the assumptions made by previous investigators have played a role in the manner of experimentation and possibly the interpretation of the results. As pointed out by Cantor and Chadwick (5) most investigators have assumed a priori a unique invariant eutectic crystallography and have set out to find it. This may have a tendency to bias results if in fact it turns out that there is no preferred crystallography between the phases. This point is illustrated quite nicely by the work of Cantor and Chadwick (3,5) on the Al-Al₃Ni eutectic along with the published comments on the work by themselves (2) and Garmong and Rhodes (14). In the original paper (3) Cantor and Chadwick claimed that their

data showed no crystallographic relationship between the two phases. Garmong and Rhodes (14) argued that within the range of experimental error the data could be interpreted to show that there was a preferred crystallography. Cantor and Chadwick (5) replied by showing that the relationship proposed by Garmong and Rhodes was not satisfied by the majority of the specimens studied by them and in a further study (3) presented a rather strong case indicating that the orientation of the aluminum rich phase was controlled by nucleation events and subsequent growth anisotropies and not by a mutual crystallographic compatibility with the Al_3Ni phase. The series of papers cited above show how the actual reported results of a crystallographic study may be biased by the investigator's presumptions. In addition, the presumption of a unique invariant crystallography gave no motivation for investigators to vary the solidification conditions in their work to any great extent even though it had been concluded in the literature by at least one author, Kraft (23), that different crystallographic relationships were evidently possible under varying solidification conditions.

Upon considering how the above mentioned factors limited the results of most previous investigations it was decided to study the solidification of a eutectic alloy while varying one of the solidification variables over a wide range of values. The possible solidification conditions which could be varied are composition, convection, temperature gradient, solidifica-

tion rate, and capillarity effects. It would aid in interpretation of results if the variation of the parameter could be easily correlated and related to any variations encountered in the eutectic crystallography. This restriction points to two variables, solidification rate and temperature gradient, both of which are easily measurable and which conceivably might have an effect on the eutectic crystallographic relationship. With this background in mind the present study was conceived and conducted.

This study of the crystallography of the lead-tin eutectic is characterized by a number of factors which differentiate it from previous work in the area. First of all the experimental solidification apparatus used, fixed the conditions of solidification to a greater extent than was possible in many previous investigations. The rate of solidification and temperature gradient in the liquid could both be measured accurately and varied independently. Also the careful alignment of the samples in the scanning electron microscope (SEM) relative to the electron beam allowed the growth directions to be measured more precisely than in the past. Finally since the orientation relationships were determined by channeling techniques in the SEM the microstructure and crystallography could be correlated directly without the addition of error as was the case previously in correlating X-ray data to independent optical measurements.

EXPERIMENTAL APPARATUS AND PROCEDURES

All experiments were carried out in the vertical solidification apparatus pictured in Figures 2 and 3. The alloys were solidified in 5 mm I.C./7 mm O.D. Vycor or quartz tubing 52 cm long. A hollow brass insert was fitted about 4.5 cm up into the bottom of the tubing. This rested on the lower copper support rod and an O-ring and clamping plate were used to make a vacuum seal at the bottom junction. At the top the upper support for the tubing was connected to the vacuum system and clamped to the tubing with another O-ring seal. A nylon plug with a hole through the center was threaded into the upper support and was tightened down to the tubing to prevent any vertical motion during a run. At the bottom a water tight seal was formed between the tubing and the cooling cylinder as pictured schematically in Figure 3. This seal must be well lubricated since it is movable and any sticking would cause variations in the rate of movement of the solid-liquid interface. Resting on the clamping plate of this seal were a hollow lava spacer and a stainless steel jacket which contained the thermocouple that regulated the furnace temperature.

The furnace was 20 cm in height and contained non-inductively wound nichrome wire heating elements. The furnace rested on a transit spacer on the top plate of the water chamber. By varying the thickness of this transit spacer and

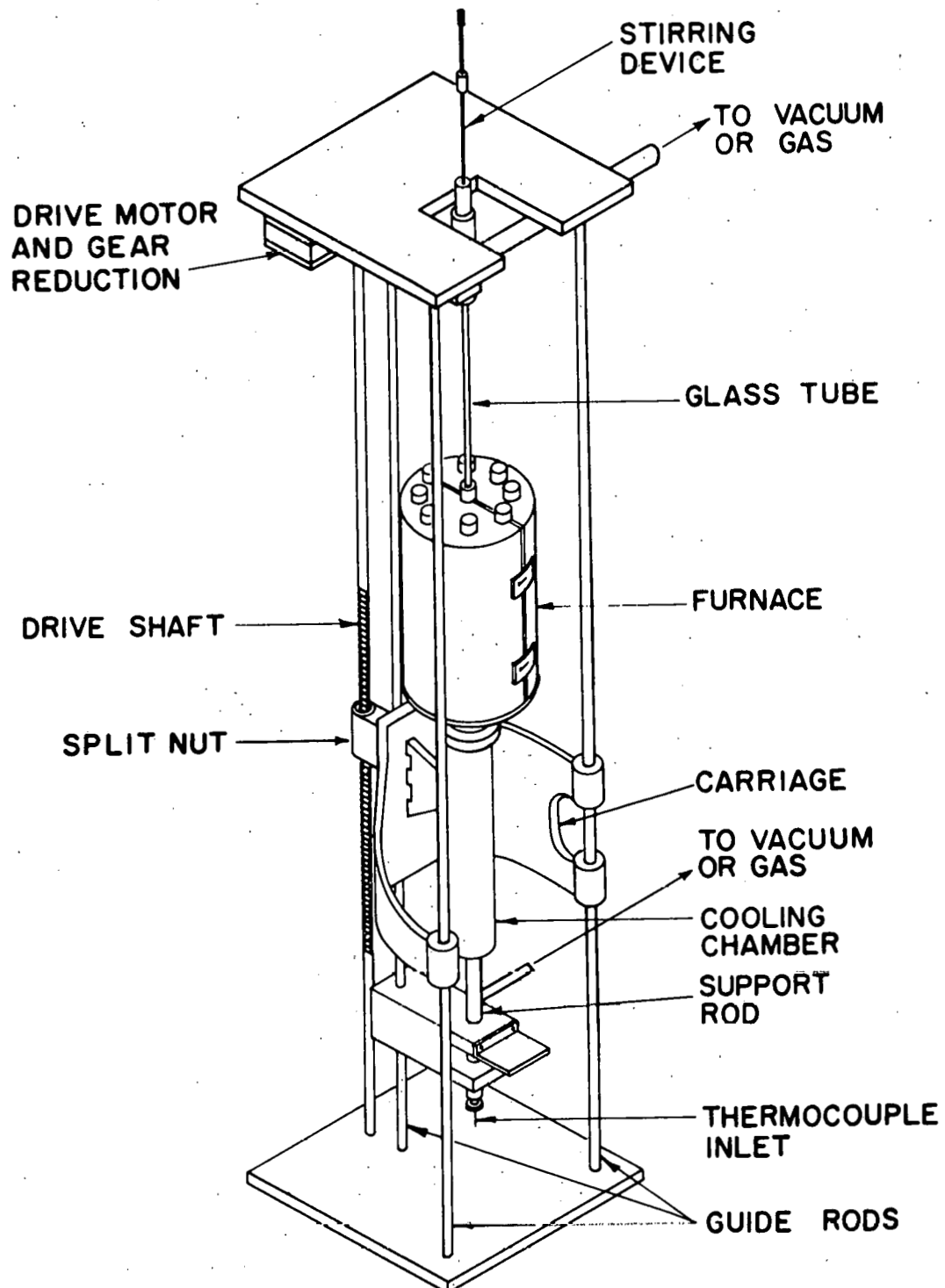


Fig. 2. An overall view of the experimental apparatus for directional solidification experiments

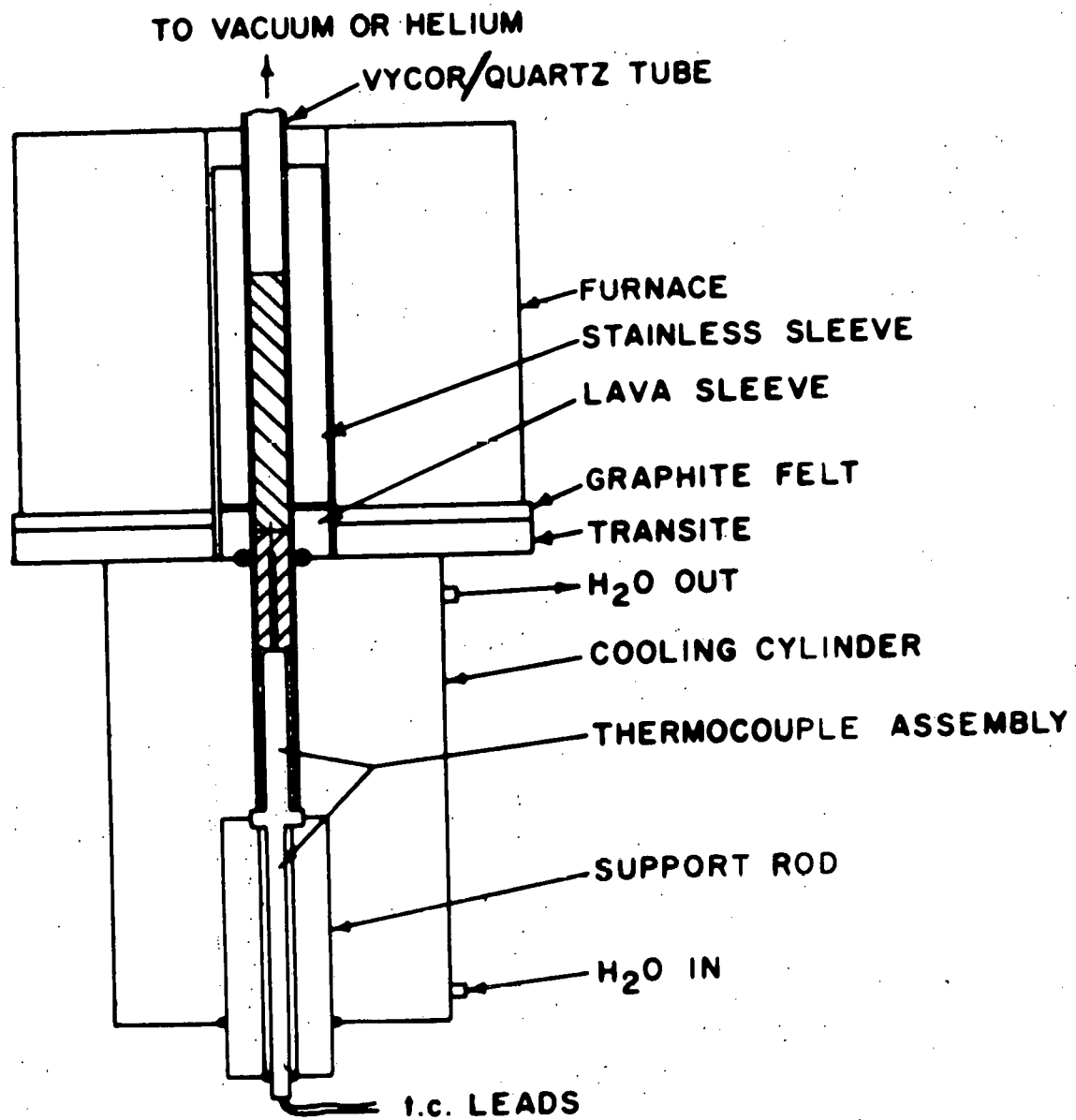


Fig. 3. A sectional view of the alloy and surrounding equipment

the lava spacer surrounding the tubing, the solid-liquid interface could be adjusted to be planar or convex at any given temperature gradient. The temperature gradient was measured by a thermocouple which extended up into the melt through the bottom copper support rod. The thermocouples were made from 2 mil chromel and alumel wires insulated from a 10 mil O.D. by 8 mil I.D. stainless steel sheath with powdered magnesia. The bead was formed by welding the end of the sheath to the chromel and alumel wires. Reaction with the lead-tin alloy during the experiments was prevented by coating the sheath with a thin layer of graphite.

The experiments were all carried out at the eutectic composition of 61.9 w/o tin. Initially a master alloy was cast starting from high purity materials: Vulcan Materials Corporation tin 99.999% pure and lead from Cominco American, also 99.999% pure. A total of about 400 g of the starting materials were weighed to within 0.01% of the desired composition. After placing the charge in a clean Pyrex crucible the crucible was transferred to a vacuum chamber. The chamber was then evacuated and backfilled with helium before final evacuation of the chamber. During the melting of the charge the pressure in the chamber was approximately 5×10^{-3} torr and remained constant. The charge was melted by a resistance furnace at about 425°C and when the melting was complete a tantalum stirring rod with a paddle attached was lowered into the melt and

oscillated to insure complete mixing. The melt was then left idle for approximately one half hour and then restirred immediately before casting. In the casting operation a bundle of 4 mm I.D./6 mm O.D. Pyrex tubes 60 mm long with one end sealed were lowered to the bottom of the melt and the system was quickly backfilled with helium thus forcing the molten alloy up into the tubes. The alloy rapidly solidified in the Pyrex tubes and the furnace was then removed allowing the system to cool. The master alloy cast in the 4 mm I.D. Pyrex tubes was then used as the starting point for all subsequent work.

After breaking the alloy out of the tubes and cleaning in acetone and methyl alcohol 40-45 g of the alloy was cut from the 60 mm long rods and placed in the apparatus described previously. The system was then twice evacuated to 25×10^{-3} torr and backfilled with helium. When refilled with helium for the final time the cooling water was allowed to flow and the furnace turned on to 400°C in preparation for the run. The first step consisted of melting down to about 1-2 cm above the bottom plug. During melting the movement of the solid-liquid interface was followed by the use of a tantalum probe and a traveling micrometer which read to 0.001". When the desired starting point had been reached the split nut was locked and the furnace and cooling jacket were allowed to travel at the predetermined rate. After about 10-15 cm of travel the run was terminated by quickly raising the cooling

jacket-furnace combination manually thus "quenching" the remaining liquid. This created an interface which was clearly evident upon macroetching and which proved useful in correlating the solidification rate data with the solidified specimen.

The temperature gradient measurements were quite simple to make. The output of the thermocouple was recorded on a strip chart as a function of time. The output recorded in this manner was essentially a straight line. Using a straight edge the slope of the line in millivolts per second could be determined. When correlated with the known temperature dependence of EMF for chromel-alumel thermocouples and the solidification rate data the thermal gradient in degrees centigrade per centimeter could be calculated. By lowering the furnace and cooling chamber manually such that the thermocouple tip was again in the molten alloy, several measurements could be made on a given experimental run. A sharp break in the thermocouple output was evident as the tip passed through the solid-liquid interface. After the desired number of measurements had been made, the run was allowed to continue and terminated as described above.

Preparation of the samples for examination began by carefully breaking the glass from the solidified specimen and macroetching the entire specimen in a room temperature etch consisting of 67 v/o glycerol, 16 v/o glacial acetic acid and 17 v/o nitric acid for approximately five minutes. This reveals the start and quench interfaces and the grain structure

of the specimen. Samples for examination in the SEM were obtained by sectioning the specimen with a jewelers saw. In all cases a surface 2 mm below the quench interface was examined. In addition two or three other surfaces nearer the start interface were examined and the microstructural features and crystallographic relationships found were recorded. After the samples were polished on a 600 grit silicon carbide wheel to obtain a smooth surface normal to the growth direction they were cleaned in acetone in an ultrasonic cleaning machine. Next they were electropolished for 1-1.5 min at 30 volts in a 6 v/o perchloric acid-methanol bath maintained at -55°C by a flow of liquid nitrogen controlled by a thermocouple in the polishing bath itself. Immediately after etching, the samples were swabbed with EDTA (a solution of ethylenediamine tetra-acetic acid disodium salt) to remove any oxidation from the lead (10) since it was found that this oxidation had an adverse effect on the quality of the channeling patterns that could be obtained from the lead lamellae. Because of the presence of a tin precipitate in the lead lamellae the electro-polishing was quite critical in that if the precipitate was not removed channeling patterns from the lead were extremely difficult if not impossible to obtain. After careful alignment of the stage in the SEM such that the electron beam and the growth direction were parallel, the surface of a given sample was examined by making two orthogonal traces of the surface carefully noting the orientations across the sample.

The crystallographic information from the selected area channeling patterns (SACPs) and the position of the lamellar interface were correlated directly by first obtaining the SACP and then lowering the specimen by controlling the height of the stage to observe the microstructure and note the position of the lamellar interface. This procedure has been shown by van Essen and Verhoeven (30) to result in an error free correlation. The orientation of the SACPs was found by comparison with an experimentally generated channeling pattern for the material in question. Upon completion of the two orthogonal traces the surface was examined at about 300X in the scan normal mode and any areas that appeared to warrant further study were also examined in the channeling mode. If only a single orientation relationship was found it was assumed to be the preferred one for the particular set of experimental conditions.

The availability of samples of Pb-Sn eutectic which were directionally solidified by previous investigators in an apparatus similar to that described above, led to a series of examinations in which the nature of their preferred crystallography was investigated. The procedure employed in solidifying these specimens differed from that described above and therefore will be summarized here. First high purity lead and tin weighed out to eutectic composition were placed in the system. Then the system was evacuated and heated to 400°C. A tantalum stirrer was then introduced into the melt and the

molten alloy was stirred vigorously to insure homogeneity. Upon completion of the stirring operation the cooling jacket was quickly raised, quenching 5 cm of the molten alloy. Then the temperature of the melt was raised to 750°C and the system backfilled with one atmosphere of high purity helium. The actual solidification of the alloy then proceeded by solidifying about 3 mm at $\sim 5 \mu\text{m/s}$ and then abruptly changing the solidification rate to the desired value which then was held constant for the remainder of the run. Electropolishing and SEM examination of the specimens followed the procedure outlined in the previous section.

In the second series of experiments the eutectic was seeded using specimens 20 mm long taken from runs grown in the first manner described above. To seed the eutectic with only the desired orientation and avoid any spurious nucleation, the samples to be used as seeds were electropolished in the same manner as before until their diameter was reduced just enough to fit into the 5 mm I.D. tubing. Using a hollow bottom plug as pictured in Figure 4 the seed was first glued to the top surface of the plug and then the assembly inserted in the tubing. Silicone rubber was introduced into the bottom of the plug and forced to flow up through the plug and around the seed and allowed to solidify. By using the tantalum probe during the melting procedure one could follow the interface movement and melt down to a point within the confines of the silicone rubber and force the eutectic to nucleate only on

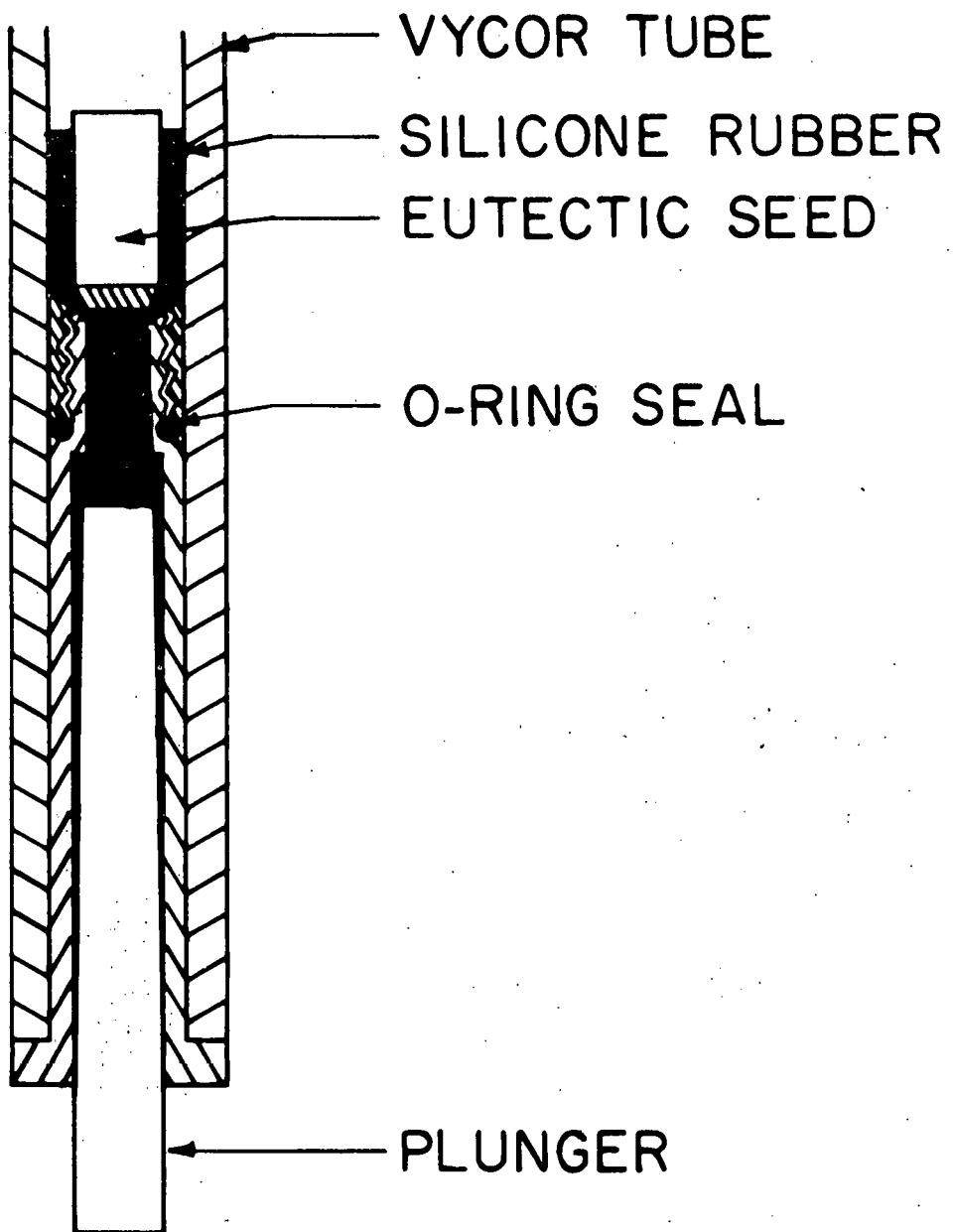


Fig. 4. Hollow bottom plug assembly

the seed as desired. Once the seed orientation was established by solidifying for about 5 cm under the same conditions that accompanied its original development, either the temperature gradient or the solidification rate was changed, and by recording the readings on the traveling micrometer the point at which the change was made could be accurately pinpointed. The primary emphasis of this phase of the experimentation was to ascertain the effect of the two variables on the lamellar spiraling found to occur in the one crystallographic mode. Most of the runs followed a simple format. After the desired crystallography was established at a solidification rate of about 20 or 40 $\mu\text{m/s}$ the solidification rate was increased in jumps of 20 $\mu\text{m/s}$ at 2.5 cm intervals until rates of 120 to 140 $\mu\text{m/s}$ were attained. At this point the remaining liquid was quenched. The runs in which the effect of thermal gradient was to be established were very similar. After 2.5 cm of alloy were solidified at 20 or 40 $\mu\text{m/s}$ and a gradient of 128 $^{\circ}\text{C/cm}$, the temperature gradient was increased by raising the furnace temperature to 750 $^{\circ}\text{C}$ where previous investigations (31) had established the gradient to be 360 ± 18 $^{\circ}\text{C/cm}$. This took approximately one hour after which the furnace was lowered slightly to melt back any of the eutectic that might have solidified during temperature fluctuations in reaching the higher gradient. Then the alloy was solidified for another 2.5 cm at the same solidification rate as before the temperature gradient change, after which the solidification rate was

increased as described above.

Measurement of the lamellar spiraling rate was done by two methods and they were cross checked on each other to insure uniformity of results. The first method was as follows: The specimen was placed on a lathe and a series of discs 1 mm thick were obtained by machining with a 0.5 mm tool bit. The specimens obtained in this manner were mounted in Quick Mount and the surfaces prepared for examination as described earlier. The lamellar spiraling rate was found by measuring the angle formed by the lamellae and a fiducial mark scribed on the specimen before machining. The second method involved an external macroetch which revealed the contrast bands noted before in the work of Hopkins and Stewart (19). The direct measurement of the spiraling rate confirmed their observation that the contrast band spacing corresponded to a lamellar rotation of 180°. As evidenced by Figure 5 the contrast bands were well defined and quite distinct particularly those at the higher solidification rates. Thus the spiraling rate could be measured by merely counting the number of bands for a given length of growth. In every case where the two methods were cross checked they agreed to within \pm 10%. Also the specimens were examined to insure that the seeded orientation was indeed the one exhibiting the lamellar spiraling effect. A series of two surface analyses were performed on the specimens exhibiting the spiraling phenomena to ascertain whether or not

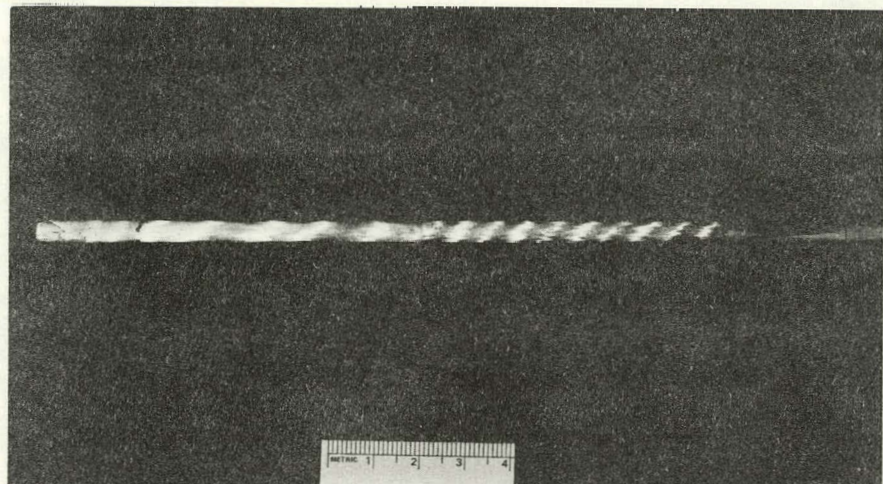


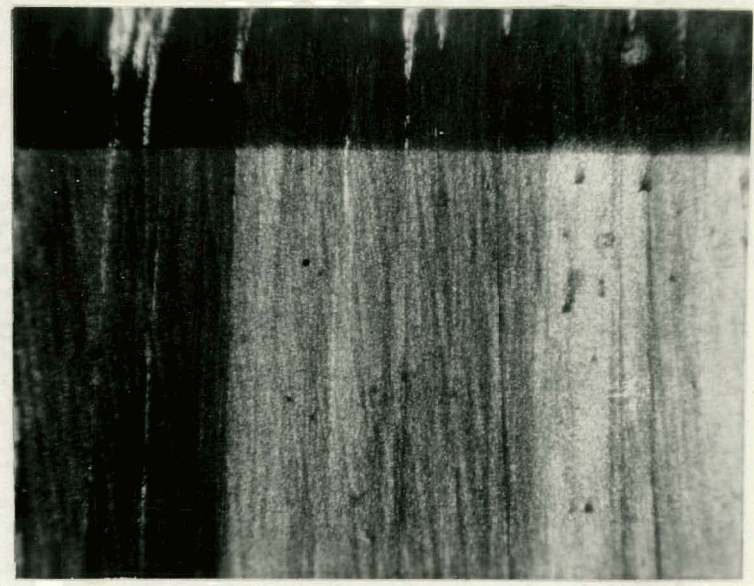
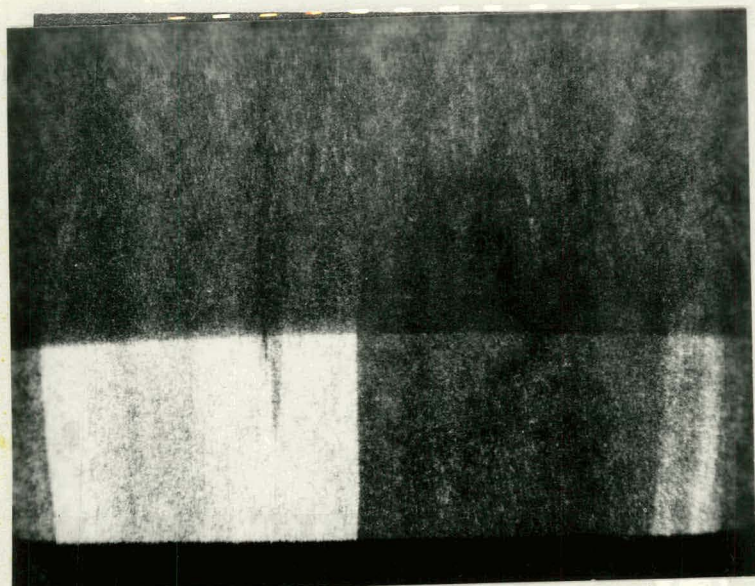
Fig. 5. Macrograph of specimen exhibiting lamellar spiraling. Growth direction from left to right. Reduced approximately 50 per cent

the lamellae were inclined with respect to the growth direction by polishing a specimen cut from a run longitudinally and examining it in the SEM. The polishing and etching were performed in the manner described above.

RESULTS AND DISCUSSION

In the measurement of the temperature gradient, G , as described earlier the lower value was found to be $128 \pm 3^\circ\text{C}/\text{cm}$. The upper gradient of $360 \pm 18^\circ\text{C}/\text{cm}$ was well established by Verhoeven and Gibson (31) in previous work and was assumed to be the same in these experiments. A comparison of the quenched solid-liquid interfaces (see Figure 6) reveals the lower gradient gave an interface that was concave with respect to the solid whereas the interface at the higher gradient is essentially planar. Thus a comparison of the results between runs with the higher gradient versus the lower one should reveal the role played by the shape of the interface, a variable which has been theorized to play a significant role in the development of preferred orientations and also subsequent steady-state lamellar rotations.

The results of the random nucleation experiments showed that the crystallography and morphology of the eutectic were highly dependent on solidification rate whereas changing the temperature gradient appeared to have little or no effect on the structure that evolved from a given set of experimental conditions. The idealized orientation relationships and experimental conditions under which they developed are summarized in Tables 1 and 2. Briefly the results showed four distinct crystallographic modes which were found to be stable at different solidification rates. As can be seen the ranges of



26

Fig. 6. Typical quench interfaces showing profile of solid-liquid interface
(a) gradient of $128^{\circ}\text{C}/\text{cm}$; (b) gradient of $360^{\circ}\text{C}/\text{cm}$. 29.1X

Table 1. Idealized eutectic crystallographic relationships found in lead-tin system

Relationship I:

Growth direction $\parallel [130]_{\text{Sn}} \parallel [1\bar{1}4]_{\text{Pb}}$
 Interface $\parallel (\bar{3}10)_{\text{Sn}} \parallel (\bar{5}\bar{3}\bar{2})_{\text{Pb}}$

Relationship II:

Growth direction $\parallel [243]_{\text{Sn}} \parallel [1\bar{1}3]_{\text{Pb}}$
 Interface $\parallel (\bar{5}\bar{1}\bar{2})_{\text{Sn}} \parallel [\bar{1}\bar{2}\bar{1}]_{\text{Pb}}$

Relationship III:^a

Growth direction $\parallel [571]_{\text{Sn}}$

Relationship IV:^a

Growth direction $\parallel [001]_{\text{Sn}}$
 Interface $\parallel (\bar{1}00)_{\text{Sn}}$

^aExperimental limitations precluded the determination of the full details of these crystallographic relationships. See text for details.

Table 2. The effect of solidification rate on the crystallography of the Pb-Sn eutectic

Run No.	R ($\mu\text{m/s}$)	G ($^{\circ}\text{C/cm}$)	Crystallography present	Length solidified (mm)	No. of grains present
34	100	128	III	155	7-10
218 ^a	100	120	III, IV	17	coarsened
213 ^a	100	120	III, IV	10	"
212 ^a	100	120	III, IV	17	"
30	98	128	III	156	---
182 ^a	51.8	260	III, II	25	---
22	51	360	III, IV	112	---
21	51	120	III, IV	106	10-15
179 ^a	46.1	360	III, II	23	---
204 ^a	44.7	120	III, IV	25	---
27	41	128	III, IV	142	2
33	41	128	II	151	10-20
20	31	360	I, II	144	---
28	21.4	128	II	155	5-10
32	21.4	128	I	170	1
35 ^a	19.1	?	II	10	---
31	10	128	I	162	20-40
163 ^a	8.5	265	I, II	75	---
55	5.7	128	I	100	2
29	5.1	128	I	153	1
143 ^a	5	?	IV, I	97	4
132 ^a	5	360	I	75	---
131 ^a	5	360	I	75	5
130 ^a	5	360	I	72	5
35	2	128	I	159	1
25	2	360	I	93	30-40
20	1.3	360	I	144	2
60	0.8	360	I	104	3

^aThe author examined the results of these runs but they were conducted by previous investigators.

stability overlap to a certain extent and a definite transition rate cannot be determined. Since the precise details of nucleation and early staged of growth will vary widely from one run to another considerable variation in the transition from one crystallographic mode to another is expected and indeed found in this work. This discussion on the results should be preceded by noting that the great majority of the data concerns the crystallography of the tin-rich phase. The reason for this is due to experimental limitations imposed by the physical nature of the eutectic. The lead-rich phase occupies only about 37 v/o at the eutectic point. Also upon cooling the lead becomes supersaturated with tin at room temperature and the lead lamellae contain a tin precipitate. These two factors limited the resolution of the electron channeling patterns (ECP) and at high growth rates ($>40 \mu\text{m/s}$) with the concomitant decrease in lamellar spacing selected area channeling patterns (SACP) from the lead phase could not be resolved under any circumstances. However relative changes in the lead phase orientation should follow those of the tin phase which is generally considered to be the controlling phase since it occupies about 63 v/o. In addition the work of Sundquist and Mondolfo (27) indicates that to homogeneously nucleate eutectic on primary lead required about 40°C of undercooling whereas nucleating eutectic on primary tin requires less than 1°C of undercooling. Studies by Davies (7) showed that the eutectic which is forced to nucleate on the

lead nucleates randomly whereas eutectic forced to nucleate on pure tin immediately forms an epitaxy with the tin substrate. Thus one would expect the tin to control the epitaxy of the eutectic.

Before plunging into the details of the findings of this study a discussion of the errors in measurement of the crystallographic parameters is in order. The measurement procedure consisted of first aligning the specimen parallel to the electron beam. Then the surface was examined in the channeling mode and in the normal mode by merely adjusting the specimen height by lowering or raising the stage of the SEM. One would expect the error in this part to be less than 1° . Thus the major source of error was in the interpretation of the spread of the data from all runs exhibiting a particular crystallographic mode. Admittedly this is somewhat subjective, however, fortuitously the data were very consistent and allowed for little error in interpretation. In any event the actual spread of the data is given when appropriate and thus the author's interpretation may be judged directly.

At growth rates less than $8 \mu\text{m/s}$ the eutectic microstructure appeared very irregular as evidenced by the SEM micrograph, Figure 7. The plates exhibited very few mismatch surfaces or lamellar terminations. Instead the lamellae branched, joined and curled in an irregular fashion. The lamellar interfacial habit plane had a mean direction that was easily determined but on a finer scale the interface had a wavy

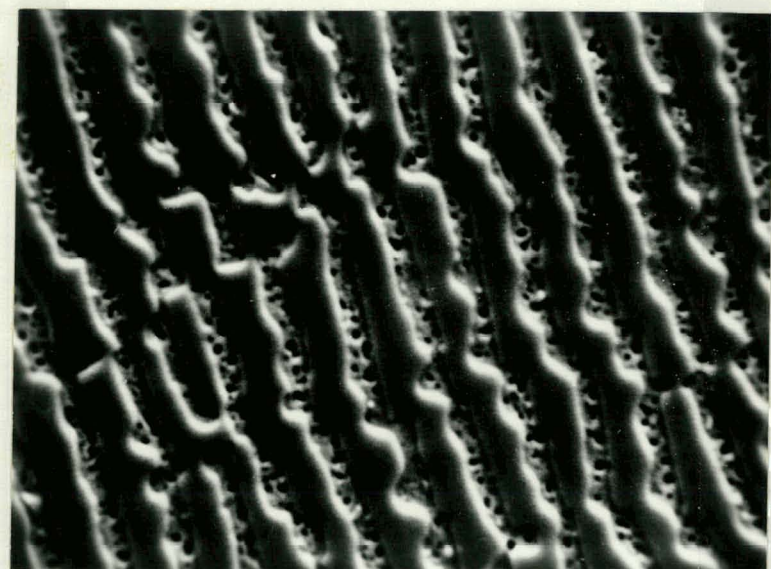


Fig. 7. Typical Pb-Sn eutectic microstructure exhibiting crystallographic Relationship I. Lead lamellae show removal of tin precipitate during etching. 2040X SEM micrograph

nature. Past investigators have termed similar structures as degenerate and have generally only considered them as transitory to the development of a low energy interface. The results of this work indicate that this is not the case here. With a convex solid-liquid interface to promote the development of the preferred orientations this structure and its accompanying crystallographic relationship which is listed in idealized form as Relationship I in Table 1 were consistently found at the indicated growth rates. Indeed this is in agreement with the results of Hunt (20) in his studies of the Pb-Sn eutectic. He found at rates of $1.3 \mu\text{m/s}$ that degenerate grains were present even after 7.0 cm of growth. It is likely the structure he observed is the one defined by Relationship I. As stated SACP's of samples grown at these rates showed a consistent crystallography but the structure was found to have regions misaligned up to 7° from the ideal $[\bar{1}30]$ tin growth direction. Figure 8 shows the range of orientations found in a typical run. A unique situation occurred in the determination of the crystallography. When attempting to index a tin SACP such as that pictured in Figure 9 an extra band was found that did not correspond to any found on the experimentally produced tin channeling maps. Subsequent work established that this was a band from a lead lamellae, thus a single SACP fixed the orientation of both phases. Figure 10, a plot of all runs exhibiting Relationship I, shows the variation in growth direction to be within 9° for all

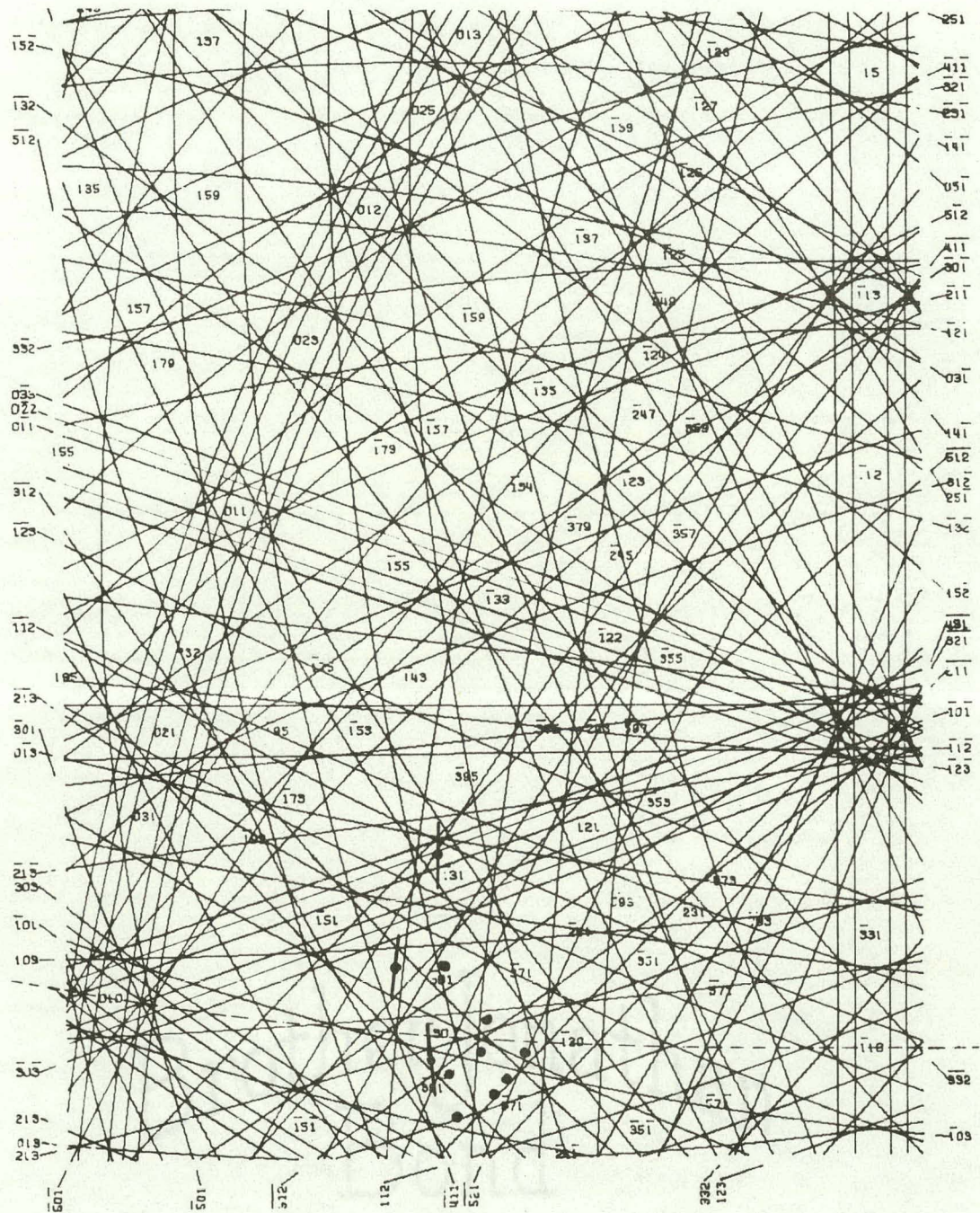


Fig. 8. Tin crystallographic data from typical run exhibiting Relationship I. Points indicate lamellar growth directions and bars the trace of the interface plane

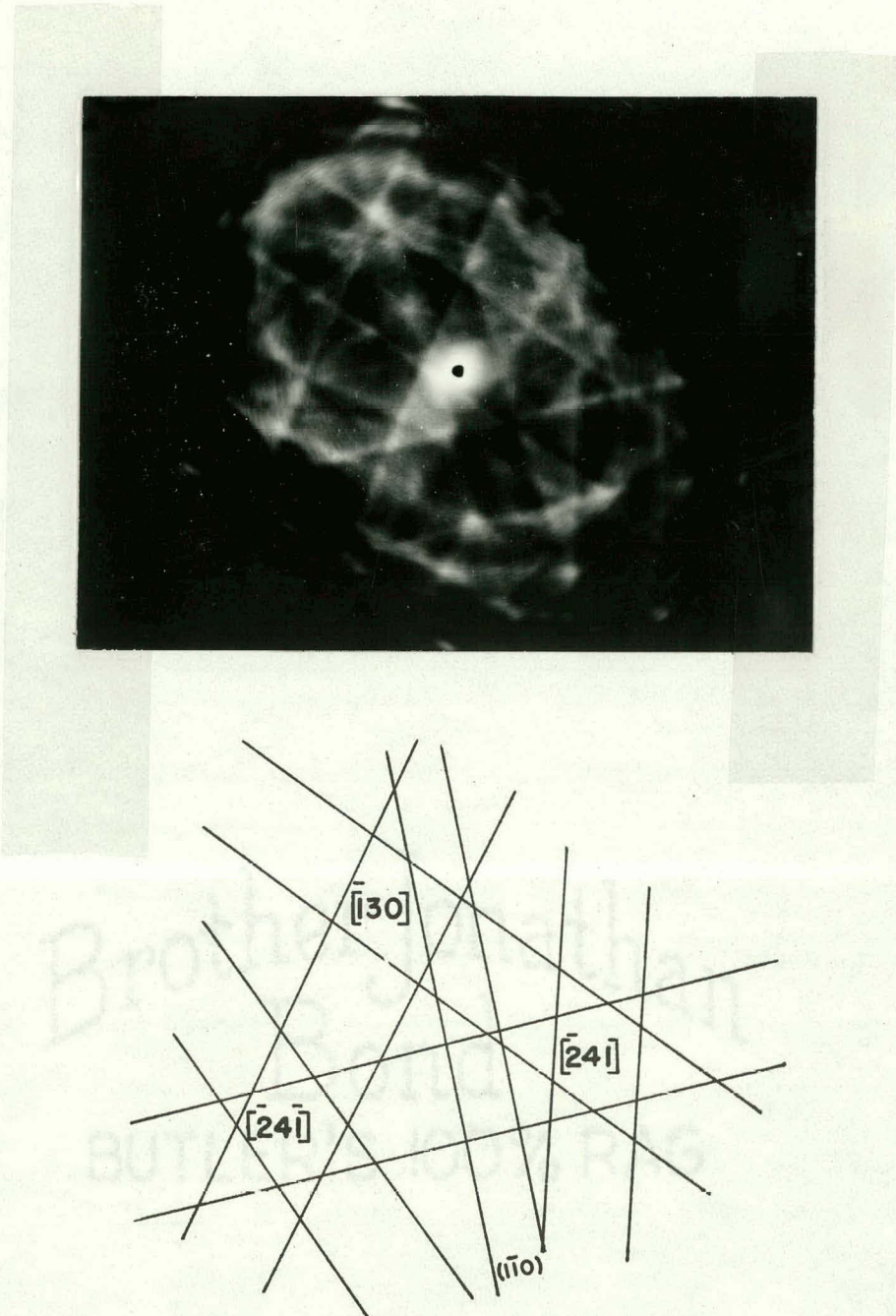


Fig. 9. Channeling pattern from a tin lamellae near the $\bar{[30]}$ pole showing a $(1\bar{1}0)$ band from the adjacent lead lamellae. (a) actual SEM pattern, (b) schematic

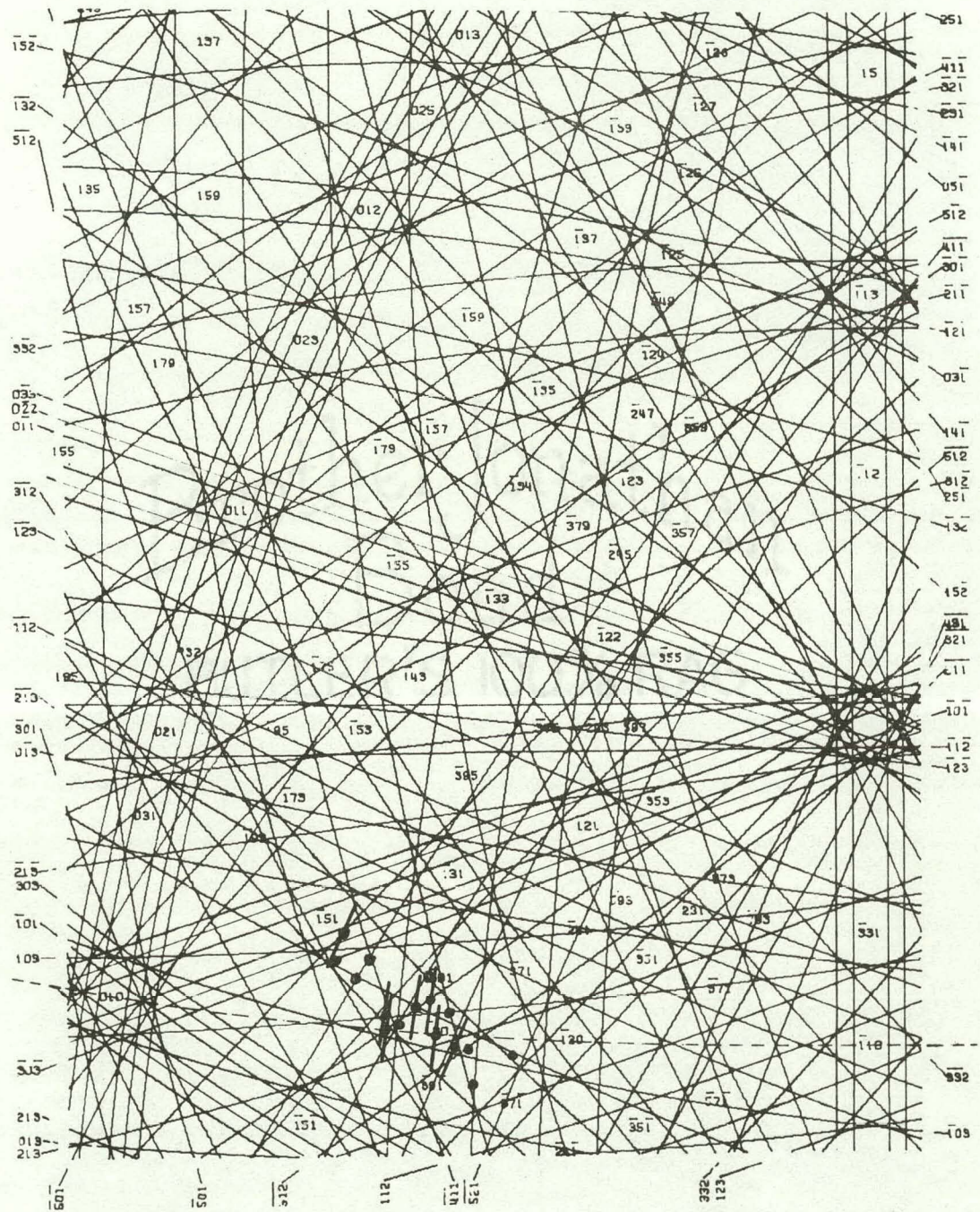


Fig. 10. Tin crystallographic data from all runs exhibiting Relationship I. Each point represents the average lamellar growth direction and interface trace from a single experiment

samples examined. Examination of runs with solidification rates of 5 $\mu\text{m/s}$ and greater indicated that the structure became more regular. The lamellae did not branch and curl wildly, instead they exhibited well defined mismatch surfaces although the lamellar interface retained its wavy nature. In spite of this increase in regularity, the crystallographic nature of the eutectic remained the same, in fact the range of misorientations for a given run became smaller when compared to that of lower rates. The morphological and crystallographic characteristics of this microstructure may be accounted for by an argument similar to that presented by Cooksey et al. (6) for the Al-Al₂Cu eutectic. It is probable at these low solidification rates the structure is controlled by the anisotropy of the growth kinetics of the tin phase. The tendency of the tin to grow in favored crystallographic direction forces the eutectic to grow with a relatively high energy interfacial habit plane. At low growth rates with attendant increase in lamellar spacing (λ) and decrease in surface area of contact between the phases, one would expect the solid-solid interfacial energies to play a lesser role in determining the eutectic crystallography. If the lamellae are growing with a relatively high energy interface the tendency to form parallel plates would be reduced and they could be expected to respond to perturbations in the solid liquid interface by branching or curling quite easily. This is exactly what was observed metallographically. The increase in regularity with increas-

ing growth rate is another manifestation of the high energy interface. As the magnitude of the perturbations inherent in the solidification apparatus becomes less and less as compared to the growth rate, the degenerate nature of the microstructure should decrease.

Increasing the solidification rate to about 8 $\mu\text{m/s}$ was found to produce a different mode of eutectic crystallography which is summarized in Table 1 as Relationship II. The morphology of this mode is what has been defined as a regular eutectic microstructure. Under all the solidification conditions that coincided with the appearance of Relationship II it maintained its regularity having well defined mismatch surfaces and lamellar faults. An examination of the SEM micrograph in Figure 11 shows that the lamellar interface is well defined and does not appear to be wavy as was found in Relationship I. For a given run this structure had less variation in the crystallography than Relationship I as can be seen by comparing Figures 12 and 8. Figure 13 summarizes the data from all runs exhibiting Relationship II. In spite of having less variation in misorientations for a given run, the range of misorientations for all runs is about 11° which is greater than was found for Relationship I. The transition to this crystallographic mode from Relationship I may be attributed to the increasing importance of the surface energy term with decrease in λ due to the increase in the solidification rate. The fact that the lamellae are more nearly parallel in



Fig. 11. Typical Pb-Sn eutectic microstructure exhibiting crystallographic Relationship II. 396X SEM micrograph

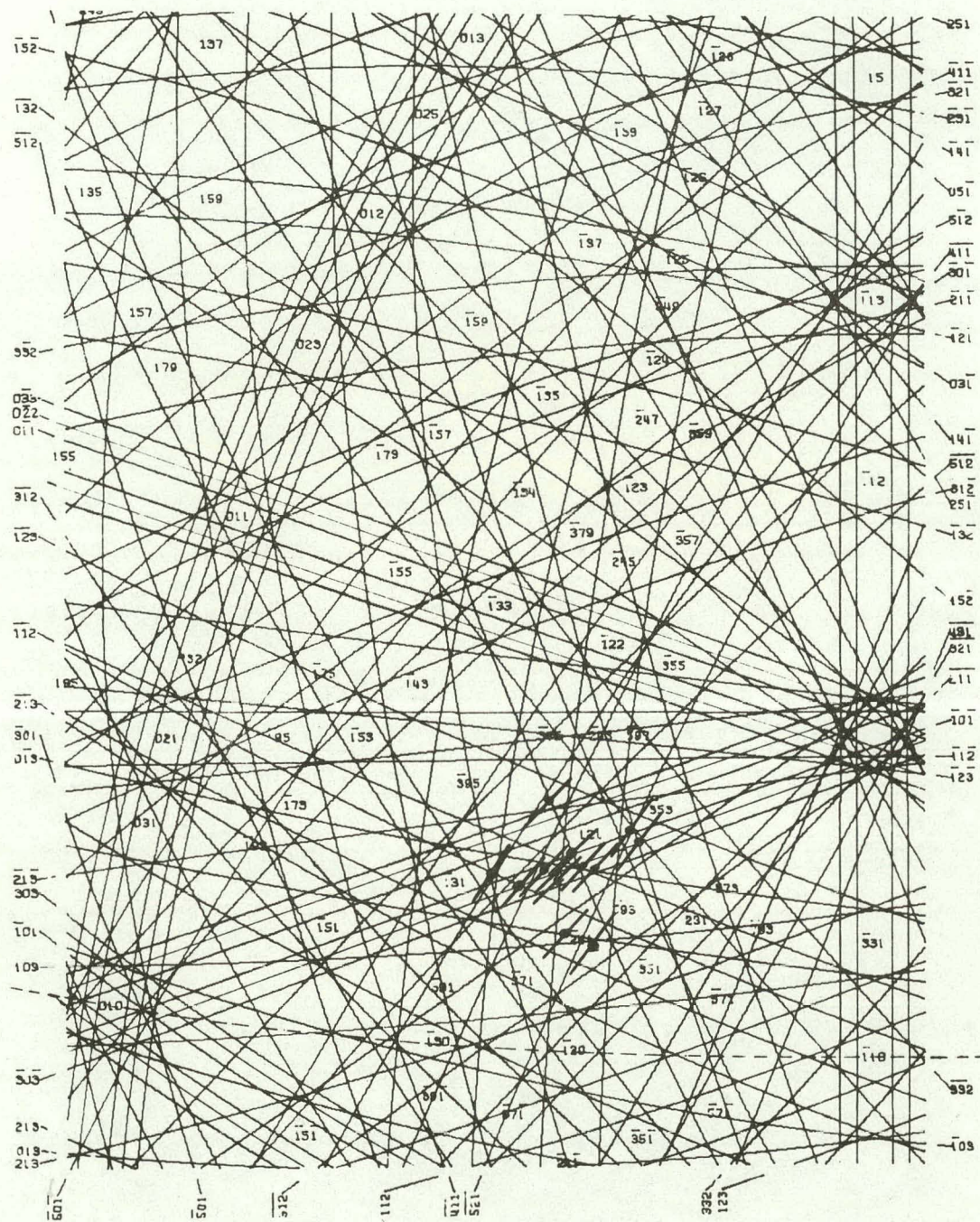


Fig. 12. Tin crystallographic data from typical run exhibiting Relationship II. Points indicate lamellar growth directions and bars the trace of the interface plane

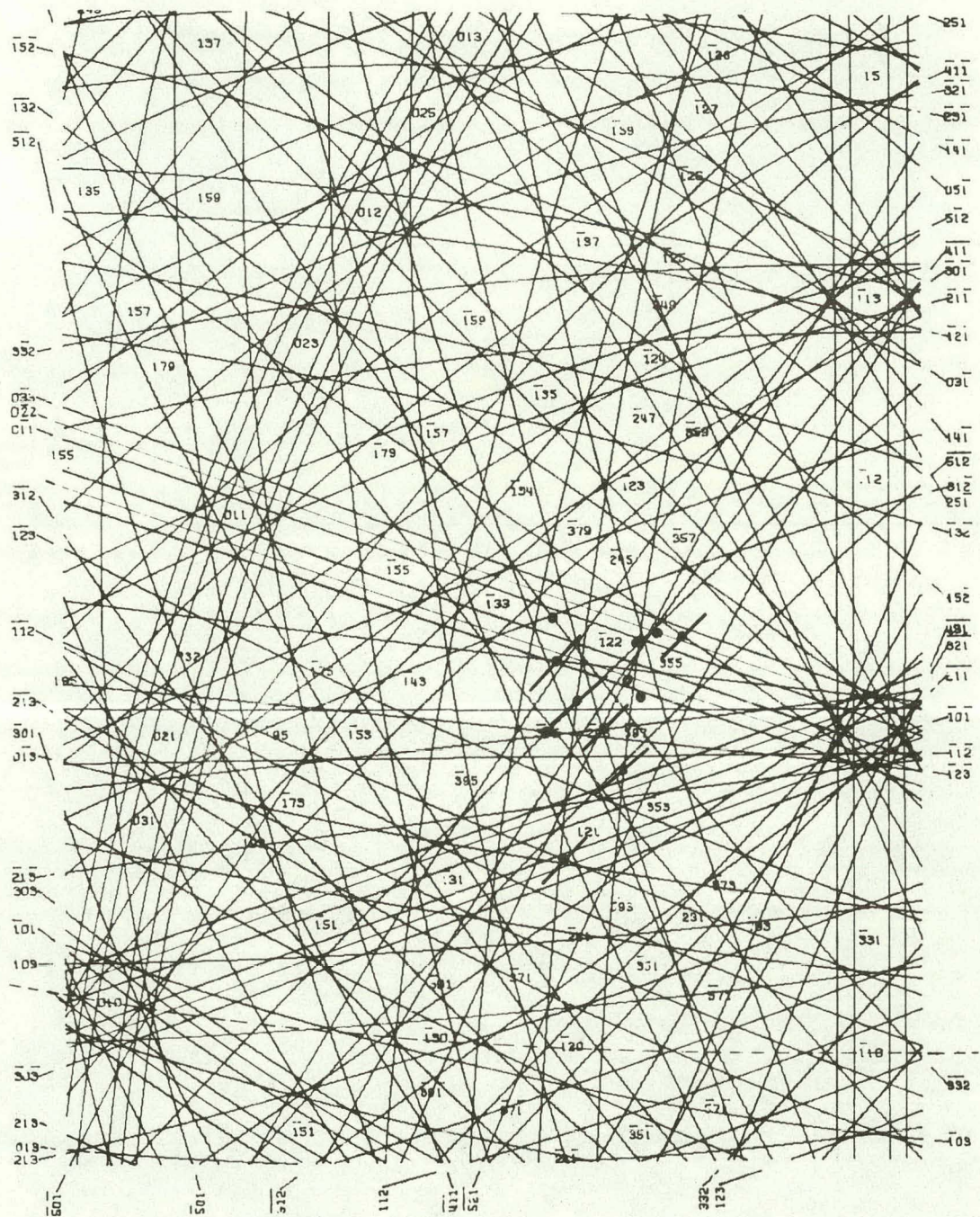


Fig. 13. Tin crystallographic data from all runs exhibiting Relationship II. Each point represents the average lamellar growth direction and interface trace from a single experiment

all cases and that the lamellar interface appears to be straight and does not have a wavy nature as in Relationship I, attest to the fact that a low energy interface is controlling the morphology. In addition by looking at Figure 13 it can be seen that the range of misorientations are such that the $(\bar{5}\bar{1}\bar{2})$ Sn plane is maintained as the average plane of contact. Thus even though the growth direction is subject to considerable variation, the low energy of the interfacial habit plane restricts misorientations that would cause a deviation from the preferred habit plane and an attendant increase in the energy of the system. Thus it appears that the experimental evidence would strongly indicate that this structure is stabilized by a low energy interface. Previous work by Hopkins and Kraft (18) in which they solidified Pb-Sn eutectic specimens in a horizontal graphite boat at solidification rates from 5.5 to 11 $\mu\text{m/s}$ under thermal gradients of 8 to 15 $^{\circ}\text{C/cm}$ indicated a slightly different eutectic crystallography than that found in the present study. Since this is one of the most cited references in the study of eutectic crystallography one is compelled to compare the two epitaxial relationships to see if the discrepancies might be resolved. To bring their proposed epitaxial relationship into equivalence with Relationship II a rotation of about 8° will bring both growth directions into coincidence and then a rotation of the lamellar interface trace of approximately 20° will yield the same habit plane as determined in this study. Within the

range of their experimental error, this shows that both studies probably found the same relative orientation of the two phases. The primary disagreement then is in the metallographic work, the growth direction and lamellar habit plane, and is not of a crystallographic nature. Hopkins and Kraft employed an X-ray technique (18) in which they correlated the crystallographic data from the X-ray work with independent observations of the growth direction and lamellar interface. The correlation of the metallographically determined growth direction and lamellar interface was done directly in the channeling work used here to determine the crystallography. By changing the height of the specimen, one could observe first the SACP and its crystallographic information and then the orientation of the lamellae in a matter of seconds. This procedure eliminated a potential source of error and provided an accurate rapid method for the correlation of the metallographic and crystallographic data (30). On the strength of this direct correlation of the data one would assume the present study to provide a more accurate statement of the relation of the crystallography to the morphology of the eutectic microstructure.

At solidification rates exceeding 40 $\mu\text{m/s}$ two quite distinct crystallographic relationships developed, not found at the lower rates. It is unfortunate that the smaller lamellar spacing occurring at these rates precluded a complete determination of the relationship since SACPs from the lead phase

could not be obtained. The first crystallographic mode, Relationship III, was a highly irregular structure similar in appearance in many respects to the morphology of Relationship I described in detail earlier. The lamellae curled and branched fairly extensively and with an irregular lamellar interface. Adjacent lamellae appeared to vary up to $3-4^\circ$ in growth direction which is a much more abrupt change in orientation than found in any other crystallographic relationship. Oddly enough the interface did not appear to correspond to any low index plane of the tin phase. The range of misorientations for all runs examined is shown in Figure 14. The second crystallographic relationship, Relationship IV, found at these growth rates generally comprised about 10-20% of the microstructure of a given cross section transverse to the growth direction. One did not need to use channeling techniques to distinguish between Relationships III and IV because of the great contrast in the morphology between the two. Microstructures exhibiting Relationship IV were generally found at grain boundaries and were extremely regular in appearance. A micrograph showing the contrast between the two structures is shown in Figure 15. Eutectic regions as described by Relationship IV occurred predominately in long thin sections with the lamellae having a sharp straight lamellar interface. The lamellae exhibited few faults but when faulted the mismatch surfaces were distinct. The growth direction and lamellar habit plane were well defined. Twenty regions examined averaged

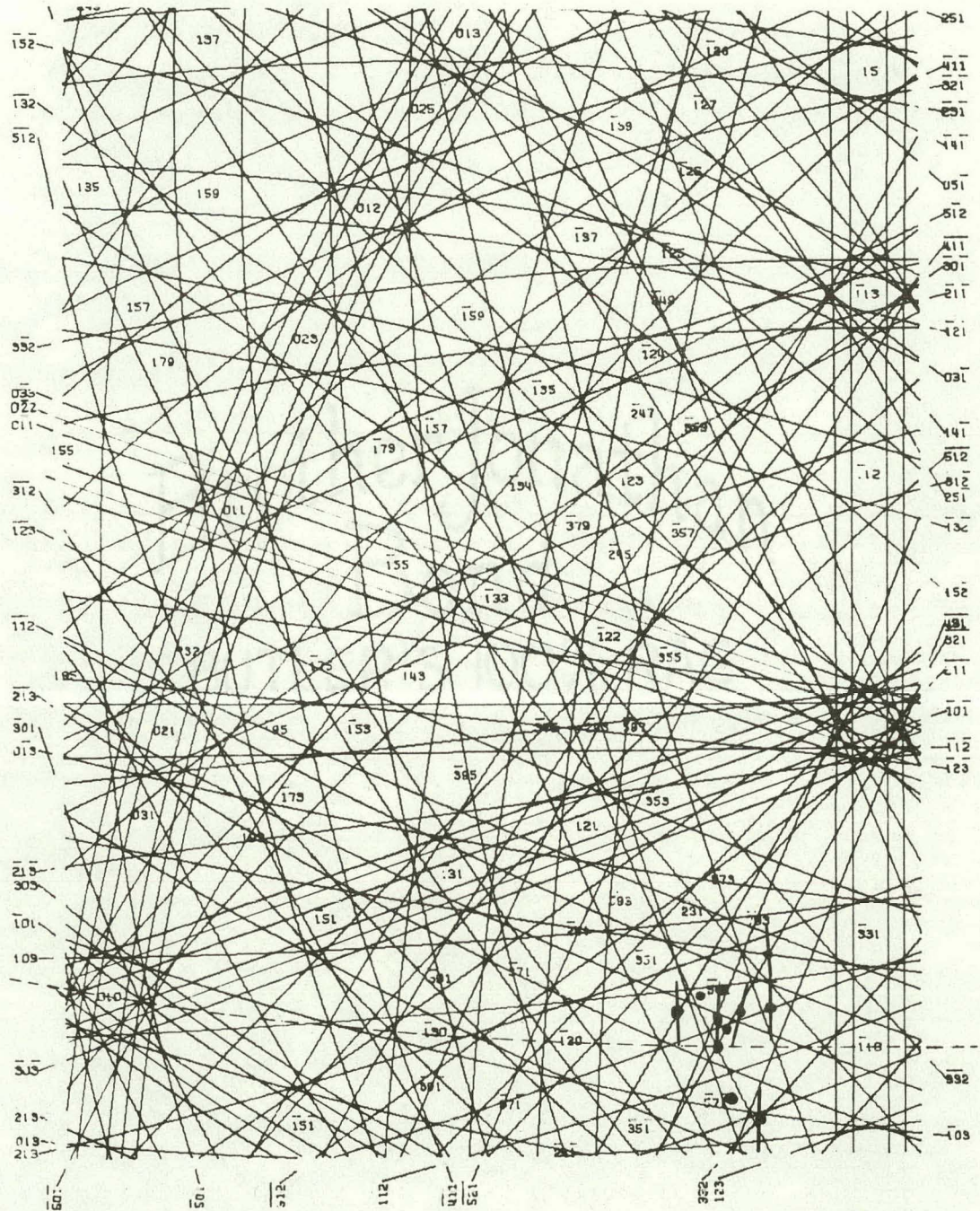


Fig. 14. Tin crystallographic data from all runs exhibiting Relationship III. Points indicate lamellar growth directions and bars the trace of interface plane

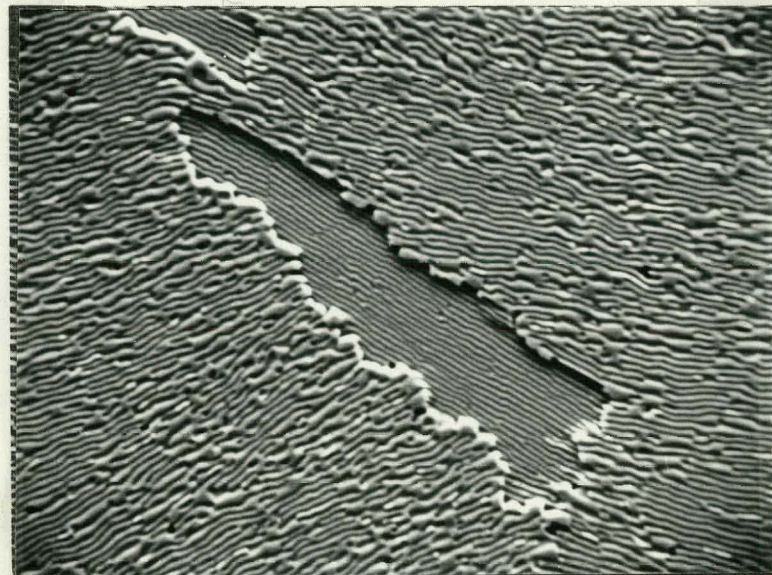


Fig. 15. SEM micrograph showing Pb-Sn eutectic exhibiting Relationship III and Relationship IV. 1000X

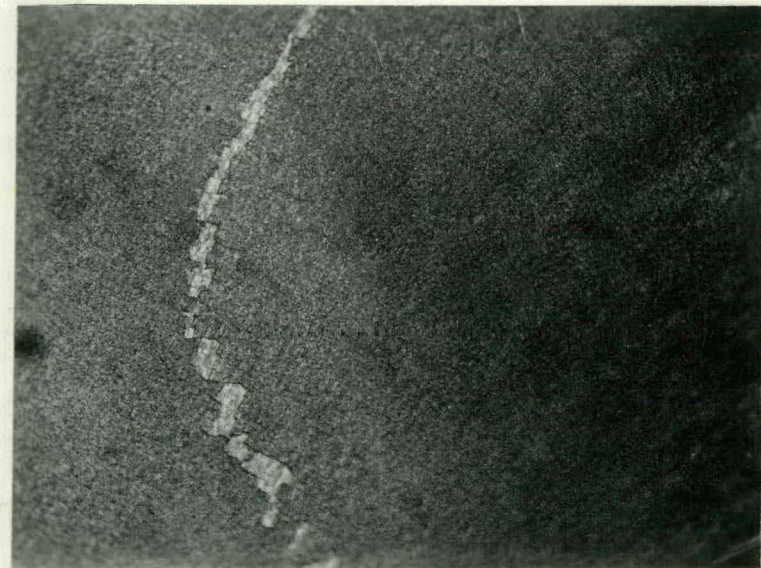


Fig. 16. Polarized light micrograph showing contrast between eutectic exhibiting Relationship III (darker areas) and that exhibiting Relationship IV (light regions). 29.1X

only about 1.8° off the [001] Sn growth direction. Since tin having a body centered tetragonal structure is optically active, polarized light microscopy was another technique which could easily be used to distinguish the two crystallographic relationships. The simplicity of this method is illustrated by the micrograph in Figure 16. Polarized light studies indicated that after the initial stages of growth the volume percentage of the microstructure characterized by Relationship IV remained nearly constant with respect to that characterized by Relationship III. The existence of a degenerate lamellar structure in the lead-tin eutectic has been observed by Hunt (20) at growth rates above $83 \mu\text{m/s}$ which is in good agreement with the findings of this study. According to Cooksey et al. (6) high growth rates favor a transition to fibrous eutectic due to the increasing importance of relative heat flow between the phases and solute redistribution. Both factors favor the radial distribution of rods versus the lamellar structure which can involve only two dimensional diffusion. Indeed this transition has been observed in many systems (6,34). Six eutectic systems were studied by Hunt and Chilton (21) in which they attempted to induce the lamellar to fibrous transition by forcing the lamellar eutectics to grow around an insert. Since the lamellae would need to bend sharply to remain normal to the interface they reasoned that the lamellae would lose their low energy advantage and that the system would break down to a rod or fibrous structure. In all systems

except Pb-Sn this is exactly what occurred. What they observed in the Pb-Sn system was a degenerate type lamellar structure which maintained an average lamellar spacing. Taken collectively these studies imply that although a transition to a fibrous morphology would not be expected one might expect some sort of modification of the lamellar structure at the higher rates as solute and heat flow become more dominant factors. With this in mind the transition of the growth direction of the tin to the [571] Sn pole is not as surprising as first thought. It may be thought of as a rotation of the tin towards the dendrite axis which is generally considered to be the [110] Sn (32) or 12° from the [110] Sn towards the [001] Sn (26) in order to accommodate the increasing heat flux. In the eutectic the tin is constrained by the maintenance of an epitaxy with the lead phase and must seek a compromise between maintaining a relatively low energy interface and the anisotropic growth of tin. The appearance of the [571] structure implies that the interface in question has a relatively high energy. The microstructure characterized by Relationship IV indicates that the lamellar interface is a very low energy interface. As stated earlier higher growth rates and the attendant decrease in λ tend to increase the importance of a low energy interface and one would expect a structure with a low energy interface to be stabilized by increasing growth rates. In light of this one might ask why Relationship IV does not predominate at high growth rates. The answer to this

is probably heat flow considerations. Since the ratios of thermal conductivities (k) for tin is $k[001]/k[110] = 0.75$ a eutectic microstructure characterized by Relationship IV would be unable to conduct the latent heat of solidification away from the advancing solid liquid interface as rapidly as one characterized by Relationship III. Thus we have two stable crystallographic relationships each a compromise of sorts under the imposed growth conditions. Relationship III is favored by heat flow considerations but has a higher energy interface. Relationship IV has a low energy interface but the importance of heat flow does not let it predominate in the microstructure. Additional evidence for the preceding explanation of the results was found in the samples from previous investigators which were examined. The specimens were annealed at room temperature for two years or more before their examination. Studies of the microstructure revealed that the eutectic exhibiting Relationship III had coarsened, that is that diffusion had occurred such that the microstructure was no longer lamellar but appeared to have coalesced into irregularly shaped patches. Eutectic characterized by Relationship IV retained its lamellar structure indicating that it had a low energy interface with little driving force to produce a coarsened structure.

Upon macroetching samples which developed Relationship II the appearance of contrast bands was immediately evident and serial sectioning of these runs confirmed that the bands were

due to lamellar spiraling about the growth direction. From the results of the microstructural and crystallographic measurements a fairly detailed picture of the phenomena was obtained. The two surface analyses performed in this study indicate that the lamellar interfaces are parallel to the growth direction and not inclined as was found in the case of lamellar spiraling in the Al-Zn eutectic by Double et al. (12). Also it appears unlikely that the lamellae are inclined in the fan like arrangement which was proposed by Double and Hellawell (11) which could give rise to the appearance of lamellar growth. What was observed was that the plates actually rotate about an axis parallel to the growth direction while the crystallography of the structure remains fixed. The most probable mechanism for this phenomena is fault movement. This idea will be discussed in depth below but for now let us review all the experimental findings before delving into possible explanations of the results. Several runs had grains which rotated in opposite directions. SACPs indicated that the sense of rotation for a given grain remained constant during growth and that it was related to the crystallography. If the growth direction of the tin was $[2\bar{4}3]$ the lamellae rotated clockwise as they grew but if the growth direction was $[\bar{2}4\bar{3}]$ the lamellae rotated counterclockwise as they grew. These findings parallel the work done by Double et al. (12) on the Al-Zn eutectic in which they correlated the sense of rotation with the nature of the lamellar habit plane. The experiments in which the growth

rate was varied clearly showed that the rate of lamellar spiraling was a function of solidification rate, see Table 3. Increasing the solidification rate (R) caused an attendant increase in the lamellar spiraling rate (ϕ) and a least squares plot of all the low gradient data up to a solidification rate of 100 $\mu\text{m/s}$ yielded the function $\phi = 5.26R + 45.05$ (see Figure 17). At solidification rates greater than 100 $\mu\text{m/s}$ the lamellar spiraling rate appeared to have reached a maximum value and showed a very slow increase beyond this point.

It should be pointed out that it proved extremely difficult to obtain spiraling rate measurements at solidification rates greater than 120 $\mu\text{m/s}$. This was due to the fact that the eutectic was seeded with Relationship II which was unstable at these rates and at growth rates greater than 120 $\mu\text{m/s}$ nucleation of new grains occurred which rapidly crowded out the seeded orientations. In every case examined these unseeded grains exhibited a crystallography corresponding to Relationship III which is additional evidence for the stability of Relationship III versus Relationship II at growth rates greater than 40 $\mu\text{m/s}$.

Using the function from above to calculate the expected spiraling rate for Hopkins and Stewart's Czochralski grown Pb-Sn eutectic samples one obtains a value of $86^\circ/\text{cm}$. This is in surprisingly good agreement with their measured values of 88 and $92^\circ/\text{cm}$ considering the differences in solidification

Table 3. Summary of the data on the effect of solidification rate (R) and thermal gradient (G) on the lamellar spiraling rate (ϕ)

Run #	R ($\mu\text{m/s}$)	G ($^{\circ}\text{C/cm}$)	ϕ ($^{\circ}/\text{cm}$)
28	21.4	128	151
33	41.0	128	259
36	1.0	128	37.5
	21.3	128	144
37	21.3	360	124
	21.3	128	135
38	10.4	128	84.3
41	20.3	128	140
	59.3	128	379
	79.0	128	462
	98.0	128	543
	117	128	566
42	40.8	128	268
	60.3	128	360
	80	128	443
	100	128	571
	119	128	584
43	41.0	128	277
45	41.3	128	313
46	41.5	128	290
	20.6	128	140
48	16.7	128	137
	81	128	459
	121	128	584
	162	128	600
50	20.4	128	167
	79	360	643
54	20.6	360	156
	41.3	360	375
	80.8	360	663
	101	360	825
	120	360	1029
55	41.3	360	257
	60.8	360	365
	80.5	360	450
	100.4	360	517
57	41.0	360	360
	60.9	360	491
	80.5	360	627
	101	360	900
59	41.3	360	263
	60.9	360	360
	80.5	360	436
	101	360	514
	120	360	568
	140	360	576

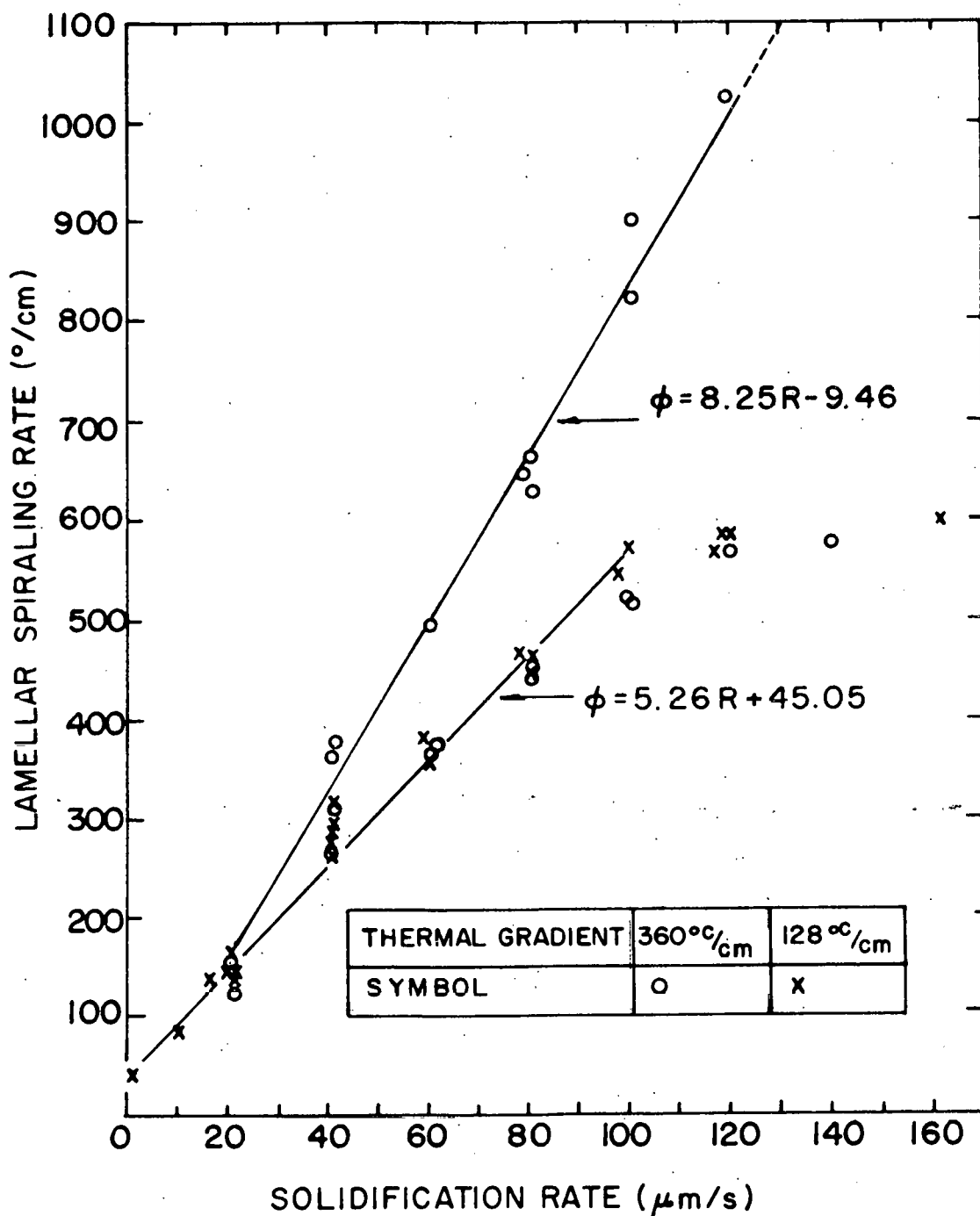


Fig. 17. Data showing the dependence of the lamellar spiraling rate (ϕ) on the solidification rate (R) and temperature gradient

conditions. The data obtained from the higher gradient experiments was somewhat confusing. Three of the experiments performed under the gradient of 360°C/cm showed a higher rate of lamellar spiraling for a given growth rate. The data yielded a linear relationship of the form $\emptyset = 8.54R - 9.46$ which was found by a least squares analysis. This finding is consistent with the work of Hopkins and Stewart in that they found that Bridgeman grown samples exhibited a higher rate of lamellar spiraling for a given growth rate than their Czochralski grown samples, which is equivalent to saying the higher gradient gave an increased rate dependence since one would expect the thermal gradients in Bridgeman technique to exceed those in the Czochralski method. However, the data from two of the high gradient runs followed the lower gradient relationship. The reason for this disparity in results was not discovered during the course of the experimentation. Since a specimen from one of the runs showing the increased dependence on solidification rates was used to seed the next one which exhibited the lesser dependence the conflict in results is puzzling. In view of the work of Hopkins and Steward one would be tempted to disregard the data showing a decreased dependence on growth rate. In any case it is clear that at least in this system the assumptions of Double et al. (12) that increasing the temperature gradient would cause a subsequent decrease in lamellar spiraling rate are in direct conflict with the experimental evidence.

A rather simple explanation of the growth rate dependence is possible. Assuming that the phenomena of lamellar spiraling is caused by fault movement biased in one direction leads naturally to two fundamental questions. First since the motion of faults biased in one direction would inevitably lead to a fault free structure, how and why are the faults regenerated? Secondly how does one explain the increased dependence on solidification rate with increasing temperature gradient? It is reasonable to assume a steady state equilibrium value of fault density for a given set of growth conditions. As the growth rate increased and the lamellar spacing became smaller the increased mobility of the faults would permit a higher rate of lamellar spiraling. At some point however the ability of the faults to move would be expected to reach a maximum value and this is exactly what was found to occur somewhere in the vicinity of 100 $\mu\text{m/s}$. It seems probable then that the rate of lamellar spiraling is dependent on the density of faults and their mobility. Previous investigations indicate that fault density is growth rate dependent. Yue (33) in his studies on the Al-Mg eutectic found fault density to be a linear function of the growth rate over a wide range of values. In agreement with this assertion is the work of Dean and Gruzleski (8,9) on the Al-Al₂Cu eutectic and that of Berthou and Gruzleski (1) on the Sn-Cd eutectic. In both cases they found a linear growth rate dependence of fault density. In addition both groups found that fault density was not a func-

tion of temperature gradient. To date no one has attempted to determine if fault density is dependent on growth rate in the Pb-Sn system. However in light of these three studies one would presume that it is. Hopkins and Stewart (19) found that Bridgeman and Czochralski samples which were grown at similar rates had nearly the same fault densities, but that the lamellar rotation rate differed by a factor of two. This indicates that the fault density in the Pb-Sn eutectic is probably not dependent on temperature gradient, which confirms the findings of the above mentioned authors (8,9) who worked in other alloy systems and that fault density alone does not govern the rate of lamellar spiraling. Taken in conjunction with the data from this study it indicates that the higher temperature gradient somehow increases the mobility of the faults and allows the lamellar spiraling to occur at a higher rate at a given growth rate. As can be seen the lamellar spiraling rate (fault movement rate) continues to increase beyond growth rates greater than 100 $\mu\text{m/s}$ for the high gradient runs, which is the rate the lower gradient data were found to have reached a critical point. This is additional evidence that the higher gradient permits a higher fault mobility. The apparent disparity in the data for the higher temperature gradient must be assumed to be due to other unknown factors affecting fault density or mobility which were not held constant between experiments. This work indicates a need for detailed work on

fault density and mobility in lamellar eutectics in order to fully understand the nature of the lamellar spiraling phenomena.

SUMMARY

The crystallographic nature of the Pb-Sn eutectic which had been previously thought to be unique and invariant has been shown to be highly dependent on growth rate. Four distinct crystallographic modes have been shown to occur and the microstructures which are characteristic of each have been identified. Cooksey et al. (6) performed a similar study of the Al-Al₂Cu eutectic. They showed a wide range of structures to be attainable in that system but failed to do a detailed crystallographic study as was performed here. Since these have been the only two successful attempts to control the microstructural and crystallographic characteristics of a eutectic microstructure one would hope that similar studies would be performed on a great number of alloy systems to ascertain the extent that crystallography of the microstructure can be controlled.

The second phase of this work was the study of the lamellar spiraling phenomena which was first discovered to occur in the Pb-Sn eutectic by Hopkins and Stewart (19). As might be expected this phenomena was characteristic of only one crystallographic mode. Some significant conclusions can be drawn from this work in regards to the nature of the phenomena. First of all, the crystallography of the eutectic remains invariant during the lamellar spiraling and the lamellae are not inclined with respect to the advancing growth

front. In addition, the rate of lamellar spiraling appears to increase with increasing growth rate or temperature gradient. This dependence is rationalized with a model that characterizes the spiraling in terms of fault movement and mobility. An in depth understanding of the phenomena is prevented by a lack of detailed studies on the variables affecting fault density and mobility. At present the work in this area is sketchy, and a clear understanding will not be achieved until additional comprehensive studies on lamellar faults become available.

BIBLIOGRAPHY

1. Berthou, P. and J. E. Gruzleski, "The Origin and Elimination of Faults in Sn-Cd Eutectic Alloys," J. Crystal Growth, 10, 285 (1974).
2. Cantor, B. and G. A. Chadwick, "Author's Reply to Comments on "The Growth Crystallography of Unidirectionally Solidified Al-Al₃Ni and Al-Al₂Cu Eutectics"," J. Crystal Growth, 30, 140 (1976).
3. Cantor, B. and G. A. Chadwick, "Crystallography of Al-Al₃Ni, Al-Al₂Cu, and Al- (AlAg) Eutectics during Nucleation and Early Stages of Growth," J. Crystal Growth, 30, 101 (1975).
4. Cantor, B. and G. A. Chadwick, "Eutectic Crystallography by X-ray Texture Diffractometry," J. Crystal Growth, 30, 109 (1975).
5. Cantor, B. and G. A. Chadwick, "The Growth Crystallography of Unidirectionally Solidified Al-Al₃Ni and Al-Al₂Cu Eutectics," J. Crystal Growth, 23, 12 (1974).
6. Cooksey, D. J. S., M. G. Day, and A. Hellawell, "The Control of Eutectic Microstructures," in Crystal Growth, H. S. Peiser, Ed., Pergamon, New York, 1967, 151.
7. Davies, V. deL., "Mechanisms of Crystallization in Binary Eutectic Systems," J. Inst. Metals, 93, 10(1964-65).
8. Dean, H. and J. E. Gruzleski, "Observations on the Details of Fault Line Movement in Lamellar Eutectics," J. Crystal Growth, 21, 51 (1974).
9. Dean, H. and J. E. Gruzleski, "A Study on the Fault Structure in the Al-CuAl₂ Eutectic," J. Crystal Growth, 19, 253 (1973).
10. Dimartini, C., "Metallographic Technique for Lead and Lead Alloys," Vol. 8, Metals Handbook: Metallography, Structures and Phase Diagrams, American Society for Metals, Metals Park, Ohio, 132 (1973).
11. Double, D. D. and A. Hellawell, "Lattice Rotations in Eutectic Crystals," Phil. Mag., 19, 1299 (1969).
12. Double, D. D., P. Truelove, and A. Hellawell, "The Development of Preferred Orientations in Eutectic Alloys," J. Crystal Growth, 2, 191 (1968).

13. Fletcher, N. H. and P. L. Adamson, "Structure and Energy of Crystal Interfaces I. Formal Development," Phil. Mag., 14, 99 (1966).
14. Garmong, G. and C. G. Rhodes, "Comments on "The Growth Crystallography of Unidirectionally Solidified Al-Al₃Ni and Al-Al₂Cu Eutectics" by B. Cantor and G. A. Chadwick," J. Crystal Growth, 30, 140 (1976).
15. Hogan, L. M., "Nucleation and Growth of the CuAl₂-Al Eutectic," J. Aust. Inst. Metals, 10, 78 (1965).
16. Hogan, L. M., R. W. Kraft, and F. D. Lemkey, "Eutectic Grains," in Advances in Materials Research, Vol. 5, H. Herman, Ed., Wiley, New York, 82 (1971).
17. Hopkins, R. H., Ph.D. Thesis, Lehigh University, Bethlehem, Pa., 1967.
18. Hopkins, R. H. and R. W. Kraft, "Nucleation and Growth of the Pb-Sn Eutectic," Trans. Met. Soc. AIME, 242, 1627 (1968).
19. Hopkins, R. H. and A. M. Stewart, "Lamellar Rotations in the Pb-Sn Eutectic," Phil. Mag., 22, 199 (1970).
20. Hunt, J. D., "The Modification of Eutectics," Ph.D. Thesis, Cambridge Univ., Cambridge, England, 1963.
21. Hunt, J. D. and J. P. Chilton, "An Investigation of the Lamella Rod Transition in Binary Eutectics," J. Inst. Metals, 91, 338 (1962063).
22. Jones, R. R. and R. W. Kraft, "The Structure of the Zn-Mg₂Zn₁₁ Eutectic," Trans. Met. Soc. AIME, 242, 1891 (1968).
23. Kraft, R. W., "Crystallography of Equilibrium Phase Interfaces in Al-CuAl₂ Eutectic Alloys," Trans. Met. Soc. AIME, 224, 65 (1962).
24. Kraft, R. W., "Technique for Determining Orientation Relationships and Interfacial Planes in Polyphase Alloys: Application to Controlled Eutectic Specimen," Trans. Met. Soc. AIME, 221, 704 (1961).
25. Labulle, B. and C. Petipas, "Crystallographic Study of the Thin Pb-Sn Lamellar Eutectic Ribbons," J. Crystal Growth, 28, 279 (1975).

26. Ohara, S., "Controlled Growth of Tin Dendrites," Acta Metallurgica, 15, 231 (1967).
27. Sundquist, B. E. and L. F. Mondolfo, "Heterogeneous Nucleation in the Liquid-to-Solid Transformation in Alloys," Trans. Met. Soc. AIME, 221, 157 (1961).
28. Straumanns, M. and N. Brakss, "The Structure of Zn-Co Eutectic," Z. Phys. Chem. B30, 117 (1935).
29. Takashi, N. and K. Ashinuma, "Direct Study of Eutectic Alloys by Means of Electron Microscopy," J. Inst. Metals, 87, 19 (1958-59).
30. van Essen, C. G. and J. D. Verhoeven, "Rotation between Micrographs from the Scanning Electron Microscope and Electron Channeling Patterns," Journal of Physics E., 7, 768 (1974).
31. Verhoeven, J. D. and E. D. Gibson, "Interface Stability of the Melting Solid-Liquid Interface," J. Cryst. Growth 11, 29 (1971).
32. Weiberg, W. C. and Chalmers, B., "Further Observations on Dendritic Growth in Metals," Can. J. Phys., 30, 488 (1952).
33. Yue, A. S., "Microstructure of Mg-Al Eutectic," Trans. Met. Soc. AIME, 224, 1010 (1962).
34. Yue, A. S., "Origin of Rod-like Eutectic," J. Inst. Metals, 93, 10 (1964065).

ACKNOWLEDGEMENTS

The road to a graduate degree has its ups and downs with many a pitfall along the way and I would like to thank all those who helped to smooth my way. In particular fellow researchers Dave Pearson and Ed Gibson provided many invaluable insights to me when I was confronted with a seemingly insurmountable experimental difficulty. Their timely advice and suggestions helped make this study a reality. Also I had the privilege of working under Dr. John D. Verhoeven whose wealth of ideas and infectious enthusiasm kept me going even at those times when everything seemed to go awry. For that no thanks can suffice. Finally a great deal of credit is due to Verna J. Thompson whose expert typing transformed my illegible handwriting into this finished thesis.